

## IDENTIFICATION OF RELEVANT BUT STOCHASTIC INPUT PARAMETERS FOR FATIGUE ASSESSMENT OF PRE-STRESSED CONCRETE BRIDGES BY MONITORING

David Sanio<sup>1</sup> and Mark Alexander Ahrens<sup>1</sup>

<sup>1</sup> Institute of Concrete Structures, Ruhr-University Bochum  
Universitätsstraße 150  
44780 Bochum, Germany  
e-mail: david.sanio@ruhr-uni-bochum.de  
alexander.ahrens@ruhr-uni-bochum.de

**Keywords:** Fatigue, pre-stressed concrete, existing bridge, monitoring.

**Abstract.** *Since in the middle of last century when most bridges were erected in Central Europe, they have reliably been in service but subjected to both continuously increasing traffic amounts and weights. Over the decades, the number of heavy-weight trucks on roads has increased and prognoses even confirm the trend to hold up for the future. Today, many of these bridges mostly made from pre-stressed concrete to grant slenderness and appealing aesthetics, have suffered from damage and need to be assessed to judge remaining bearing capacities. Here, especially fatigue is often of concern. Generally all structural materials are involved, concrete, reinforcement and high-strength steel of tendons are prone to fatigue; pre-stressed bridges highly rely on the compression forces induced. Notably, also pre-stressing of concrete has been enhanced from its early beginnings. However some of the older bridges possess deficiencies originally unknown when erected.*

*The reference structure available for research, a multi-span hollow-web girder of around 300 m length, has been built field-wise requiring intermediate joints to couple the tendons. These joints are in danger of cracking since reinforcements provided according to former code versions at the times of erection do not meet nowadays demands. If the joints crack, concrete releases tensile forces left to be borne by the tendons only. Consequently, stress amplitudes caused by traffic rise significantly along with the fatigue damage induced per load cycle. Damage progress is usually tracked employing S-N-curves and Miner's rule. It is known that uncertainty in the stress amplitude is magnified by the S-N-curve with respect to the number of cycles to failure [1]. To determine stress amplitudes in a tendon one can measure strains in-situ by structural monitoring or predict its size by numerical simulation [2]. Both alternatives highly depend on the quality of input data [3, 4]. Hence, the focus has been set to determine the most relevant contributors to precisely predict remaining structural lifetime.*

*Among the scattering input variables assessed by sensitivity analyses are geometrical, material and load parameters, whereas the latter ones turned out to be decisive. Advice to match the findings with structural monitoring measures scheduled for existent bridges is given.*

## 1 INTRODUCTION

Today, many bridges in Central Europe are 40 years old or even older. Since times of erection the loads and load frequencies have increased significantly while degradation progresses. Additionally new insights have been gained and today such a structure would not be built exactly the same. Especially regarding fatigue of pre-stressed concrete bridges, older designs of coupling joints exhibit certain structural weakness.

Within the scope of a research project at the Institute of Concrete Structures of the Ruhr-University Bochum funded by the German research association (DFG) a more than 50 years old bridge was equipped with monitoring elements and examined in detail. By a lot of different measures, like testing of material samples, calibrations, load analyses etc. the knowledge about the structure was increased significantly and the residual structural lifetime regarding fatigue could be estimated as accurate as possible. Finally, the results of the best-case calculation have been compared to directly measured strain-amplitudes. These amplitudes were gained by strain-monitoring on the pre-stressing strands which were opened for this reason. The measurements lasted for about six weeks under traffic. By means of sensitivity analyses the driving parameters of fatigue prognoses have been identified and ranked.

## 2 REFERENCE STRUCTURE

The reference structure “Pariser Straße” (Fig. 1) in Düsseldorf, Germany, was a single girder post-tensioned concrete bridge of around 300 m total length and built field-wise in 1959/60. The 12 spans with varying lengths between 19.9 and 32.2 m connected the city centre of Düsseldorf with the German highway system (Autobahn). At the northern end, the bridge branched into a smaller part and a longer one, which was decommissioned shortly after the construction phase. The fix point (FP) was situated at the centre of the bridge in axis VII, where the building process also started. Due to the field-wise construction, the pre-stressing tendons were connected at coupling joints about one-fifth of the belonging span-length where the bending moment from steady loads was supposed to be almost zero.

The prestressing tendon profile was piece-wise parabolic according to the bending moment expected with additional tendons close to the columns. In this part the cross-section was haunched and ended in a cross girder right above the columns.

Because of discovered cracks in the coupling joints the bridge was strengthened by steel columns, which were placed near the coupling joints in 1977 and 1992. This had relevant impact on the structural behaviour and led to significantly smaller stresses in the joints and hence almost eliminated the fatigue problem in hindsight. Of course, this effect was unknown at the beginning of the project.

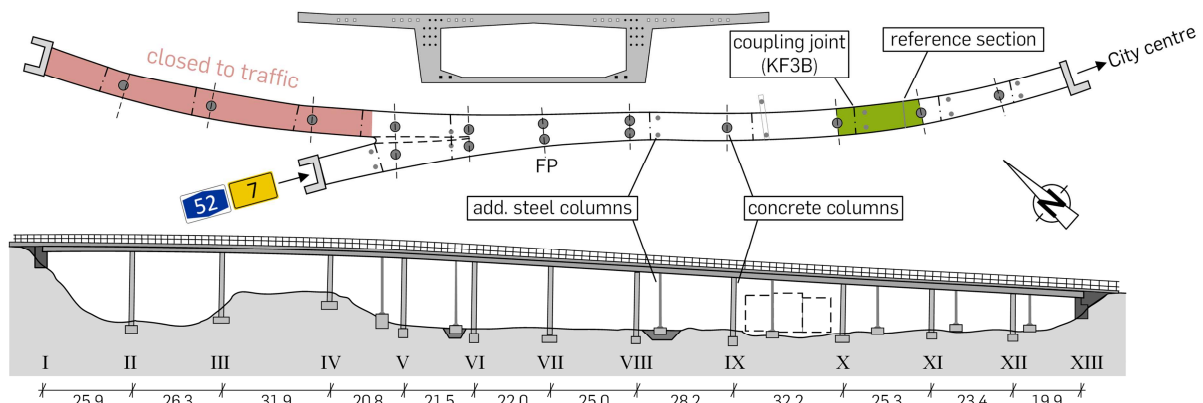


Figure 1: Reference structure “Pariser Straße” in Düsseldorf.

In order to determine the accuracy of lifetime predictions the cracked coupling joint was focussed on, equipped and a lot of measurement data was evaluated. Additionally, a similar reference section without couplings in the same span one-fifth from the next column, which was considered to be non-cracked, was monitored. All measurement strain data which has been collected in this section was smaller than that in the coupling joint.

### **3 APPROACH TO FATIGUE SIMULATION**

The fatigue lifetime was determined in consecutive steps. At first, the internal forces were determined with a Finite Element (FE) program, stresses and fatigue in an external spreadsheet calculation. To gain a computational model, the structure was idealised for simulation in InfoCAD 14 (InfoGraph) software, using beam elements for the compact box-girder. The elements possess 6 degrees of freedom per node (3 translations and 3 rotations). The pre-stressed tendons are implemented as individual truss elements. Along the entire bridge, five similar main-groups of tendons could be identified and combined. In the proximity of the columns additional slightly curved tendons were included separately. Since only a single span of the bridge and especially its coupling joint was considered for monitoring the computational model was reduced as well. The first seven spans (axes I to VIII in Fig. 1) were excluded and idealised by equivalent springs (cf. [2]). Hence, the span of interest and two more to each side were modelled and used for simulation. Besides, the spring-stiffness was calculated on a simplified model of the entire bridge (without haunches and pre-stressing). Comparative calculations proved that influence to be small with respect to the considered part. Even a rigid support provided adequate results. Certainly, time-dependent effects like creep and shrinkage were considered in the FE-model.

Relevant load positions for the different truck types to be applied were determined by influence lines. Two different types of fatigue traffic loads were assessed; the fatigue load models (FLM) 3 and 4 according to EN 1991-2 (cf. Section 4.3).

The computation of stresses was performed separately preserving the internal equilibrium conditions for the cross-sections of interest. So, relevant parameters could be assessed and evaluated in detail. For the estimation of fatigue lifetime, S-N-curves and Miner's rule were used for damage evaluation and accumulation. In cases of the time-dependent effects and hence always variable stress-ranges the linear accumulated damage could not serve directly for the calculation of the fatigue lifetime by inversion, but by numerical simulation until fatigue failure at  $D = 1.0$ .

### **4 MONITORING MEASURES AND SIMULATIONS FOR FATIGUE ASSESSMENT**

A bunch of different monitoring measures were performed on the reference structure. For a time period of about four weeks strain measurements ran under traffic. Afterwards, the monitoring continued for about four weeks without traffic, in order to eliminate external influences. In this situation and also during deconstruction of the bridge, specimens were taken to determine material data in experiments at the institute's facilities. The main elements of the monitoring are shown in Fig. 2 and will be shortly summarised in the remainder.

#### **4.1 Calibration of the structural model**

By means of different material measurements and load tests, the calculation model was calibrated. First, an initial FE-model was developed, based on documentation data and construction plans. Material data from concrete and steel (pre-stressing steel and reinforcement) were determined from samples, which were taken from the structure. Cores have been drilled from

both concrete types, a B300 ( $f_{ck} = 20 \text{ N/mm}^2$ , nominal value) which was used for the deck slab and a B450 ( $f_{ck} = 28 \text{ N/mm}^2$ , nominal value) for webs and the bottom slab. Both, the compressive strength and the Young's modulus were determined in tests and transformed to initial values (after 28 days) employing a standardized method provided in EN 1992-1-1. By a time- and cement type-dependent exponential coefficient time-variable values could be calculated. As can be seen from Fig. 2 (top left) the measured average value of the compressive strength was much bigger than expected from nominal data. Based on the experimental tests the scatter could be reduced (nominal standard deviation  $\sigma = 5 \text{ N/mm}^2$ , standard deviation from measurements  $\sigma = 3,4 \text{ N/mm}^2$ ).

With respect to the mean value of the Young's modulus the tendency was vice versa. For the concrete B300 the mean values were also higher than expected, but its scatter increased due to a small statistical sample size ( $n = 7$ ) and embedded rebars in particular samples, although their influence could be eliminated by specific methods.

Additionally, specimens of the pre-stressing steel were tested in the laboratory for its static parameters (ultimate tensile strength, Young's modulus). An individual S-N-curve was determined for the tendons ( $\varnothing 26 \text{ mm}$ , St80/105), (top centre in Fig. 2), cf. [5].

For the estimation of time-dependent and instantaneous losses one tendon was cut nearby a strain gauge. So, the remaining pre-stress could be determined directly by the reduction of strain measured (Fig. 2, top right). Since only one tendon was cut, this could not give a general value but a specific one. Here, the loss of pre-stress (61 %) was significantly higher than calculated (about 24 %) (cf. [6]).

The influence of other uncertain parameters like the stiffness of the columns and the foundations as well as the pressing force of the additional steel columns (Fig. 1) could be determined by a load test. Therefore, a truck with known axle loads was placed on specific load positions. By geodetic deflection measurements and strain monitoring the structural response could be determined. In an iterative optimisation process the difference between measured and calculated deflections was minimised and finally a calibrated FE-model generated (bottom left of the calibration part in Fig. 2).

## 4.2 Temperature monitoring and simulation

In accordance to previous research projects, the temperature has a relevant impact on the fatigue behaviour [7]. So, a temperature monitoring with an accompanying numerical simulation of the temperature fields was performed as well.

For temperature monitoring six sensors were placed in the concrete, spatially distributed over the cross section: two in each web and one in deck- and bottom-slab. The air-temperature inside and outside the concrete girder was measured with two additional sensors. Since temperature can be considered constant over the length of an almost straight structure, only one cross-section was equipped for monitoring and simulation. Each hour ( $f = 1/3600 \text{ Hz}$ ) the temperature was determined for more than eight weeks. The measured values were used for the calibration and verification of the simulation routine.

The numerical temperature simulation was performed employing a specially developed routine, which calculates non-linear and non-stationary temperature fields based on daily local climatological data, which is available for free from the German National Meteorological Service (Deutscher Wetterdienst, DWD). The calculation is based on general, numerical temperature simulation approaches for bridges already proposed in the literature [8, 9, 10]. The temperature distribution inside a solid body can be calculated by the heat transfer  $\Delta Q_{i,in}$  from Eq. (1) given in numerical form, where  $\Delta t$  is the time step (its selection depends on the element's size and the material data, cf. [8]),  $\dot{q}_{i,k}$  denotes the heat flow density and  $b_{i,k}$  the con-

tact length between the rectangular element  $i$  and a number of  $m$  surrounding elements indexed with  $k$ .

$$\Delta Q_{i,in} = \Delta t \sum_{k=1}^m \dot{q}_{i,k} b_{i,k} \quad (1)$$

The heat flow density inside a solid body can be determined with a linear approach of the thermal conduction (Eq. (2)), which depends on the two lengths  $l_i$  and  $l_k$  of both adjacent elements, their thermal conductivities  $\lambda_i$  and  $\lambda_k$  and temperatures  $\vartheta_i$  and  $\vartheta_k$  to the current time instant.

$$\dot{q}_{i,k} = \frac{2 \lambda_i \lambda_k}{\lambda_i l_k + \lambda_k l_i} [\vartheta_k - \vartheta_i] \quad (2)$$

More challenging is the integration of climatological effects which are considered by specific boundary conditions. First, the heat transfer at the cross-section's surface is handled in a similar way as before, but one adjacent element is replaced by the heat transfer at the boundary  $r$ .

$$\Delta Q_{i,ext} = \Delta t \left[ \sum_{k=1}^m (\dot{q}_{i,k} b_{i,k}) + \dot{q}_{i,r} b_{i,r} \right] \quad (3)$$

The heat flow density at the boundary  $\dot{q}_{i,r}$  can be determined analogue to the internal one acc. to Eq. (2), but the temperature of element  $k$  must be substituted by an equivalent air-temperature  $\vartheta_{air,eq}$ . Additionally, the heat-transfer coefficient  $\alpha$  must be considered. Here, different relevant external effects like solar radiation, air temperature, wind, reflections etc. can be gathered and integrated to the simulation by an equivalent air-temperature. For details on the determination of the equivalent air-temperature see e.g. [9, 10].

$$\dot{q}_{i,r} = \frac{2 \alpha \lambda_i l_{i,r}}{2 \lambda_i + l_i \alpha} [\vartheta_{eq,air} - \vartheta_i] \quad (4)$$

The most relevant parameter for the fatigue simulation is the linear vertical temperature gradient  $\Delta T_v$ , which can be calculated directly from the temperature field. It enters the FE computations as part of the fundamental steady loads.

$$\Delta T_v = \frac{h}{I_y} \int_A \vartheta(y, z) z dA \quad (5)$$

The parameters in Eq. (5) are the height of the cross-section  $h$ , its moment of inertia  $I_y$ , its area  $A$  and the temperature  $\vartheta$  at each point based on a coordinate system with the origin in the centre of gravity. For numerical application the formula can be expressed by Eq. (6). Here, the surface integration of temperature and the vertical position are replaced by the sum of all temperatures and the vertical position of the corresponding elements  $i, j$  and their areas  $A_{i,j}$ .

$$\Delta T_v = \frac{h}{I_y} \sum_i \sum_j \vartheta_{i,j} z_{i,j} A_{i,j} \quad (6)$$

Based on local climatological data of the bridge (Düsseldorf, Germany) the temperature fields were simulated for the monitoring period and compared to the measurement results at the specific points. A good agreement of measured and simulated results was found. Afterwards and based on this routine as well as comprehensive climatological data sets since 1970,

a time series of the vertical gradients was generated for more than 40 years. Then it was reduced to a histogram of gradients (Fig. 2, right). In comparison to other evaluations as given in [7, 11] the shape looks slightly different. This is probably due to the unique geometry, position (height and orientation) and location of every bridge. Hence, an individual and more realistic assessment of the temperatures can obviously be reached by such a simulation.

In order to evaluate the general effort of detailed temperature gradients, a general temperature histogram for box-girders according to the German guideline for recalculation [11] was assessed in comparison to the “ordinary” approach according to EN 1991-2 employing constant gradient. Already this enhancement led to an increase of the fatigue lifetime of about 90 %. By contrast assessing the bridge-specific local gradients collected, the fatigue lifetime turned out slightly smaller. Due to seldom extreme but decisive gradients the results at the reference structure were impaired. However, that must not be a general conclusion for other locations.

### **4.3 Assessment of load models**

A back-transformation of the monitoring results to the number of axles, the load per axle and the distance between them is not possible based on the monitoring results in this case. In the meantime other research projects achieved significant progress in this field, see [12, 13]. For an assessment of current fatigue load models the two general alternatives of EN 1991-2, FLM 3 and 4 (Fig. 2, right) were evaluated. Since FLM 3 consists of four single loads, 120 kN each, it is a simplification and underestimates the fatigue lifetime significantly. Hence, the more detailed model FLM 4, which consists of five trucks with different numbers of axles and individual axle loads, was evaluated. It claims to represent the general European traffic more realistic, if such an idealization is possible at all. With it, the fatigue lifetime could be increased about 400 % at the reference structure (cf. [4]). Herein, the change of the relative frequency of each truck, which also changes with time, is included in agreement with the assumptions of [11]. The effort of even more detailed load models (more than five fully-loaded standard truck types) can be estimated, if the fatigue lifetime based on monitoring data (which represents the real traffic) is considered as in section 4.5.

### **4.4 Evaluation of traffic counts for a load history**

The load frequency was initially assumed to be constant in time, according to EN 1991-2. As a more detailed and more realistic approach the total amount of trucks per year was determined evaluating the results of traffic counts since 1970. A trend function was calculated and combined with the relative frequencies of the five single trucks (cf. section 4.3) to estimate the fatigue lifetime. In sharp contrast to the global trend, the number of trucks per year at the reference structure decreased and increased the lifetime four times. Further details are given in section 6.

### **4.5 Direct strain-monitoring**

Additionally, strains of the pre-stressed steel were measured for several weeks by strain-gauges which were applied directly to the tendons. Therefore, concrete was removed in small areas around the tendons, ducts laid bare and opened. Strain gauges were applied to two tendons in the coupling joint and in the similar – but not cracked – reference section. Three strain gauges were applied to each section for redundancy and to measure both tendons in the lower layer. Strains were measured for four weeks under traffic and further four weeks without traffic to determine other influences like temperature and externally induced vibrations.



Even if stresses are close to zero, an evaluation with the lower branch of the S-N-curve shows a trend of monitoring benefits. In addition to the “best-case” calculation, which is represented by the measures in the previous steps (sections 4.1 to 4.4), the monitoring result for the fatigue lifetime differed from simulation by about 40 %. That amounts an additional increase of the fatigue lifetime of about 430 % in comparison to the initial model (Fig. 2, left).

## 5 SENSITIVITY ANALYSIS FOR SPECIFIC PARAMETERS

For detailed evaluations of the fatigue calculation regarding influences of specific material parameters the calculation process is repeated employing scattering parameters. Only probably relevant material parameters are considered.

In order to reduce the number of simulations, relevant load conditions were determined in advance. Since FLM 4 represents the real traffic much better than FLM 3, all five trucks are considered. For simplification time-dependent effects are neglected and the conditions fixed to the times of monitoring ( $t = 53$  years). This leads to a slight but safe and here negligible underestimation of the lifetime, since the absolute values are of minor interest. The focus is set on the sensitivities.

Since the additional steel columns reduced stresses nearly to zero, the situation without these columns is numerically simulated. Additionally, only those time-intervals, when the linear vertical temperature gradient falls below  $\Delta T \leq -5$  K, have turned out to be most relevant for the coupling joint of interest. Temperature gradients smaller than -8 K are generally neglected since they have occurred only two times in the temperature history (cf. section 4.2). Altogether 20 different stress ranges were determined resulting from 40 distinct load situations (max. and min. stresses (2) caused by each truck (5) combined with all temperature gradients (4)). The calculation can be summarized as follows:

- Since only small stresses are expected, the internal forces were determined on a linear elastic model and then the basic load was superposed for every load situation separately
- Stresses  $\sigma_i$  are determined for the cross-section using the internal equilibrium conditions
- For each stress range  $\Delta\sigma_i$  the number of load cycles until failure  $N_i$  is determined based on S-N-curves
- The applied number of load cycles  $n_i$  and Miner’s rule give the damage  $D$  acc.to Eq. (7)

$$D = \sum \frac{n_i}{N_i} \quad (7)$$

- For simplification the theoretical structural lifetime is finally calculated with Eq. (8)

$$T_{L,max} = D^{-1} \quad (8)$$

For the sensitivity analyses relevant parameters are assumed to scatter one at a time and belonging fatigue lifetime is calculated separately. Each analysis comprises 100 realizations of every single parameter employing the statistical properties summarized in Table 1.

In each diagram (Figs. 3-6) the fatigue lifetime simulation is presented based on stochastic input parameters on vertical axes. These input parameters were generated based on the inverse probabilistic distribution. The corresponding frequency distribution is qualitatively also shown on the vertical scale. The result of each simulation is a fatigue lifetime which is plotted on the horizontal scale. Hence, each point in the diagram is one simulation result as a combination of a realisation of the input variable and the corresponding output. To quantify the impact on the fatigue lifetime, histograms were generated, which summarise the results and



reveal the scatter of the output. For example, the smallest value for the concrete strength generates the shortest fatigue lifetime. Due to the higher impact of the parameters in the latter diagrams, their horizontal scale is logarithmic.

parameter	mean value	standard deviation	distribution type	additional information
pre-strain $\varepsilon_{pm}^{(0)}(t=\infty)$	1.065 ‰	0,3 ‰	normal	
vertical position of the considered tendons $z'_{p5}$	1.31 m	0.008 m	normal	
geometry:				
width of the deck slab $b_{ds}$	4.95 m	0.30 m	normal	“steering parameter” for geometry-values ( $A_c$ , $I_y$ etc.)
= moment of inertia $I_y$	0.98 m <sup>4</sup>	0.0168 m <sup>4</sup>		
concrete parameters:				
compressive strength $f_{cm}$				correlated to Young’s modulus because of the stress-strain relation acc. to EN 1992-1-1
concrete in deck slab (B300)	38 N/mm <sup>2</sup>	4,9 N/mm <sup>2</sup>	normal	
concrete in web and bottom slab (B450)	45 N/mm <sup>2</sup>	4,9 N/mm <sup>2</sup>	normal	
fatigue parameters:				
gradient of 1 <sup>st</sup> branch $k_1$	3	0,2	log.-norm.	
gradient of 2 <sup>nd</sup> branch $k_2$	7	0,5	log.-norm.	
knee-point $\Delta\sigma(N^*=10^6)$	120 N/mm <sup>2</sup>	16 N/mm <sup>2</sup>	log.-norm.	

Table 1: Parameters for the sensitivity analysis.

From the results shown in Figs. 3 - 6 a basic difference can be read: Geometrical and concrete parameters have an even smaller impact on the fatigue lifetime than the fatigue parameters that define the S-N-curve and the residual pre-strain  $\varepsilon_{pm}^{(0)}(t=\infty)$ . Since, the value of the compressive strength  $f_{cm}$  of the two different concrete types (which also affects the correlated Young's modulus in the simulation), the vertical position of the lower tendons  $z'_{p5}$  and the geometry lead to a quite smaller scatter in fatigue lifetime (coefficient of variation ( $CV \leq 0,1$ ), than the fatigue parameters and the pre-strain ( $CV \geq 0,4$ ).

Here, stress-level and stress-range determine the influences of each parameter. This becomes apparent if two simple cases are compared: All stress-ranges are below the knee-point  $\Delta\sigma(N^*=10^6)$  of the S-N-curve – as in most real cases and in the presented simulation – hence the gradient  $k_2$  is decisive and  $k_1$  has no impact (thus not depicted). If only stresses above the knee-point occur,  $k_2$  has no relevance. If the section is surely not cracked and linear-elastic behaviour holds true completely the influence of the pre-strain is small and almost zero (Fig. 2). But, the pre-strain is decisive in transition to cracked conditions (decompression state) if non-linear stresses appear and then reduces the fatigue lifetime significantly (cf. Fig. 6 and [3]). Some of the chosen 40 relevant load situations exceed the decompression state. Here, the uncertainty of the pre-strain is decisive for the fatigue lifetime and reduce it to about 7 % of the average value.

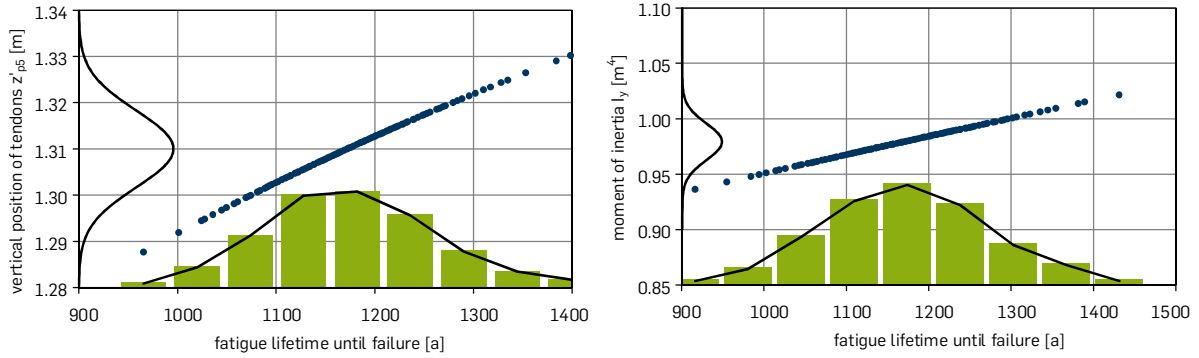


Figure 3: Sensitivity analyses of the fatigue lifetime for scattering geometry parameters.

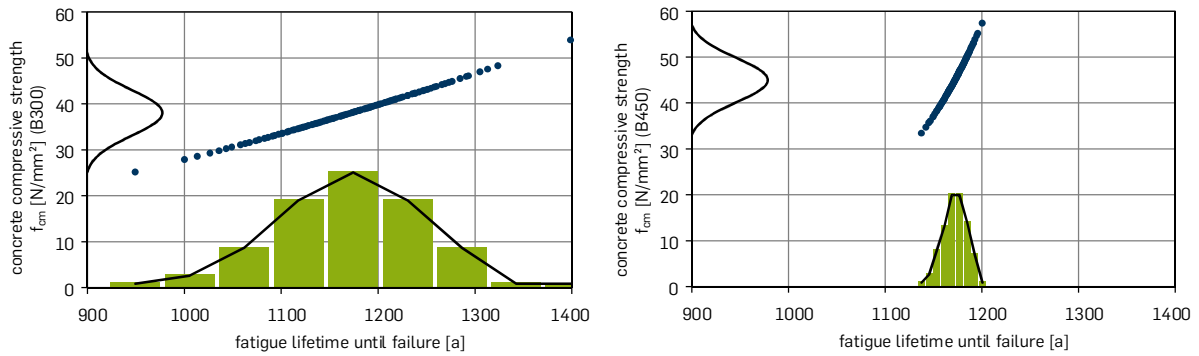


Figure 4: Sensitivity analyses of the fatigue lifetime for scattering material parameters of the concrete.

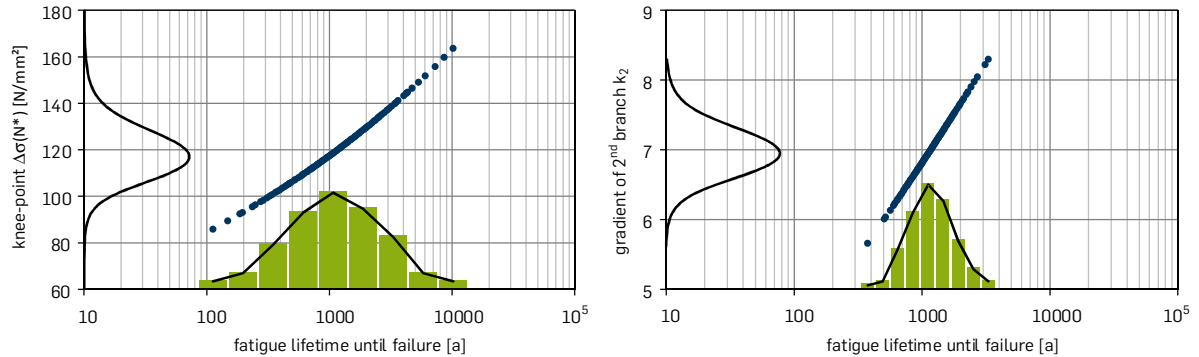


Figure 5: Sensitivity analyses of the fatigue lifetime for scattering parameters of the S-N-curve.

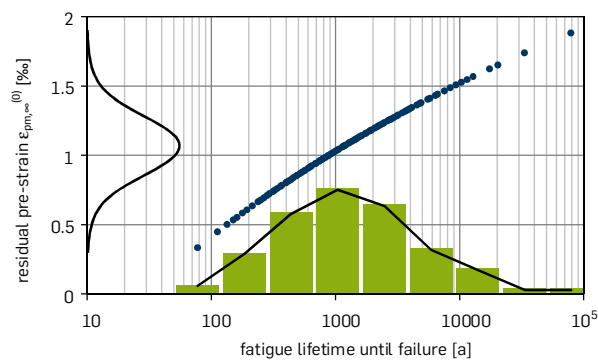


Figure 6: Sensitivity analyses of the fatigue lifetime for scattering pre-strain.

## 6 COMPREHENSIVE LOAD-HISTORY FOR THE BRIGDE

In order to determine the impact of the loads as accurate as possible a comprehensive load-history was determined for the reference structure. The procedure is shown in Fig. 7 and will be explained below.

First, the load histogram from traffic monitoring served with video-based analyses to assign relevant stresses to truck crossing events (highlighted in part 1 of Fig. 7) as explained before in section 4.5. That way, the total number of trucks could be derived also.

Second, due to a new bridge being built aside traffic limitations were imposed on the reference structure. Consequently, the total number of trucks was significantly smaller than in the year before (2011). For almost entire 2011 automatic traffic counting data was available; but unfortunately not for 2012. Missing daily data (malfunction of detectors) was interpolated according to current trends and the particular day of the week (fewer trucks at the weekend). Next, the stress-range histogram was scaled by the total number of truck load-cycles in August 2012 to the value measured in August 2011 (blue in part 2, Fig. 7). Again, daily values could not have been used for upscaling, because the Rainflow algorithm does not account for time-sequential data. In a next step the monthly distribution was scaled equivalently to the remaining months (green) and finally to one year (grey in part 2, Fig. 7).

Third, due to time dependent effects, the impact of traffic loads increased within the time [4]. Based on time-dependent structural analyses (creep, shrinkage and hardening of concrete) considering the five standard trucks of FLM 4 another unique but time-variable scaling factor was derived. At first, individual stress ranges were calculated for each year since erection as well as for the upcoming 50 years extrapolating the time-effects (part 3a, Fig. 7). However, basically the increase of stresses occurs in the first ten years after erection. Next, based on the five predictions of progress with time, a common scaling factor was generated (part 3b, Fig. 7). Since its standard deviation nearly vanishes it is seen adequate for all five courses and stress-ranges in the histogram (part 1). So, the time-dependent evolution of the load-values is also obtained by upscaling.

Fourthly, the time-variable number of the load cycles was considered employing traffic count data from three spots nearby the bridge, which were provided since 1970: At all places sets of daily manual counting data were collected over the years. These have been extrapolated to yearly values by Düsseldorf's traffic department. Since vehicles could not depart in between the spots, these local trends deliver quite accurate estimates of real traffic amounts. Next exponential smoothing of missing values and extrapolation to the future was performed (part 4, Fig. 7). A local decreasing trend appears which is in great contrast to nowadays global traffic trends. It is traced back to local effects of urban road and traffic management e.g. relocation of heavy industries nearby.

Finally, time-dependent stress ranges and traffic amounts were combined, to determine a highly accurate and complete load-history for the reference structure (part 5, Fig. 7). While load effects increase, due to creep and shrinkage, their quantity decreases locally. This results in interaction in the damage calculation, where both, loads and frequencies have a relevant impact.

For assessment, the fatigue lifetime is calculated for six situations (A-F) listed in Table 2. It clearly demonstrates the need and potential benefit of an individual load history. Please note: Since the measured stress ranges were small due to additional supports, all calculated lifetimes are only theoretical values and unrealistic to be expected for real structures. However, the results show the high impact of the very different parts of fatigue lifetime prediction and its sensitivity qualitatively. If certain steps are simplified or even neglected, the fatigue lifetime can increase or decrease manifolds.

situation	considered steps (acc. to Fig. 7)					theor. fatigue lifetime [a]
	1	2	3	4	5	
A	✓	✗	✗	const.	✗	$5.9 \cdot 10^6$
B	✓	scaled to 1 month	✗	const.	✗	$1.1 \cdot 10^6$
C	✓	✓	✗	const.	✗	$7.7 \cdot 10^5$
D	✓	✓	✓	const.	✗	$6,6 \cdot 10^5$
E	✓	✓	✗	✓	✗	$6,5 \cdot 10^5$
F	✓	✓	✓	✓	✓	$1,1 \cdot 10^6$

Table 2: Theoretical fatigue lifetime acc. to Fig. 7, if specific steps are considered.

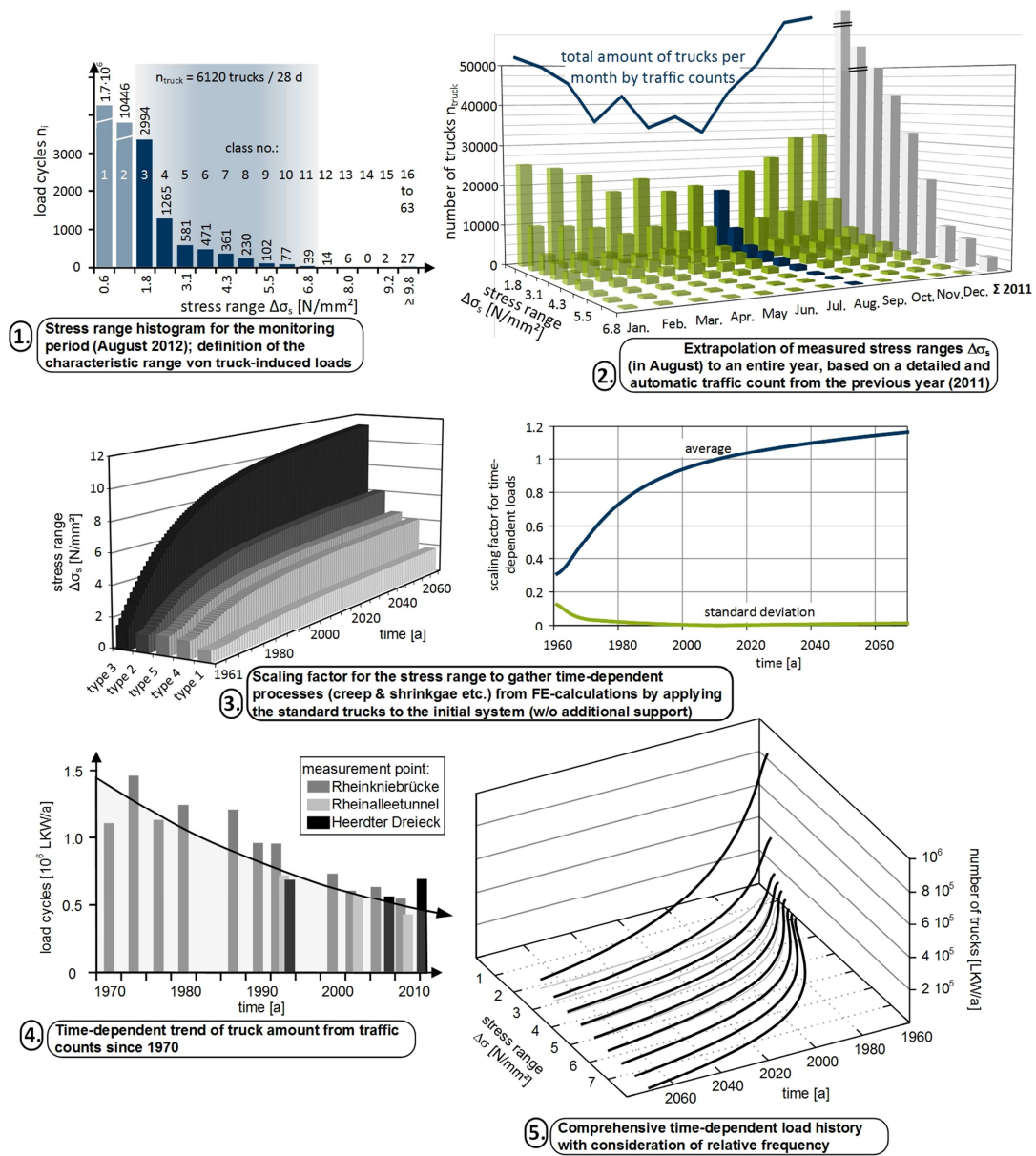


Figure 7: Steps for a comprehensive load-history at the reference structure.

## 7 CONCLUSIONS

In view of a world-wide growing stock of existent bridges to be timely judged by engineers with respect to individual damage states, remaining bearing capacities or residual lifetimes, prediction methods gain increasing importance. Therefore, politics and responsible authorities demand precise information to base economically efficient and safe decisions.

As with all kinds of forecasts of future behaviour and prospective events engineers must deal with numerous sources of inherent uncertainties in information, data, geometry, construction materials as well as computational models that idealize reality. Using these to predict the future it is utmost important to know the driving parameters, their properties and impact on the final result. In this framework the contribution treats the complex and highly relevant case of fatigue lifetime predictions of existing pre-stressed concrete bridges. At a known fatigue hot-spot of a real reference structure located in Germany comprehensive measurements by means of long-term monitoring, numerical simulation and accompanying experiments in the institute lab have been performed to deliver information on the structure and its health state. Employing stochastic analyses of the prediction method based on S-N-curves anchored in current codes, the single parameters contribution on the residual lifetime could be separated and quantified. It is shown how uncertainty already existing in the input propagates through the model, is changed herein and affects the final result. Instructions are derived which parameters should be measured at best, what assumptions can be taken and how they influence the prognosis.

## 8 REFERENCES

- [1] M.A. Ahrens, Precision-assessment of lifetime prognoses based on SN-approaches of RC-structures exposed to fatigue loads. A. Strauss, K. Bergmeister, & D.M. Frangopol eds. *Proc. 3rd Int. Symposium on Life-Cycle Civil Engineering (IALCCE 2012)*, p. 109, Wien, Austria, October 3rd-6th, 2012.
- [2] K. Bergmeister, P. Mark, M. Österreicher, D. Sanio, P. Heek, A. Krawtschuk, A. Strauss, M.A. Ahrens, Innovative Monitoringstrategien für Bestandsbauwerke. K. Bergmeister, Fingerloos, J.-D. Wörner eds. *Beton-Kalender 2015 (1), Abs. VII*, Ernst & Sohn, Berlin, 315-459, 2014.
- [3] D. Sanio, M.A. Ahrens, P. Mark, Detecting the limits of accuracy of lifetime predictions by structural monitoring. A. Chen, D.M. Frangopol, X. Ruan eds. *Proceedings of the 7th International Conference on Bridge Maintenance, Safety, Management and Life Extension (IABMAS)*, 416-423, Shanghai, China, 2014.
- [4] D. Sanio, M.A. Ahrens, P. Mark, Accuracy of lifetime predictions by fatigue monitoring. A. Cunha, F. Caetano, P. Ribeiro, G. Müller eds. *Proceedings of the 9th Int. Conference on Structural Dynamics (EURODYN)*, 2279-2286, Porto, Portugal, 2014.
- [5] Sanio, D., Ahrens, M. A., Mark, P., Rode, S., Increasing the accuracy of lifetime prediction by structural monitoring of a 50-year old pre-stressed concrete bridge, *Beton- und Stahlbetonbau* 109, 128-137, 2014.
- [6] D. Sanio, Genauigkeitssteigerung von Lebensdauerprognosen durch Monitoring einer Spannbetonbrücke. R. Breitenbücher & P. Mark eds. *Tagungsband des 54. Forschungskolloquiums des Deutschen Ausschusses für Stahlbeton (DAfStb)*, Bochum, Germany, 2013.

- [7] K. Zilch, M. Hennecke, R. Buba, *Kombinationsregeln für Ermüdung - Untersuchung der Grundlagen für Betriebsfestigkeitsnachweise bei Spannbetonbrücken*, Forschung Straßenbau und Straßenverkehrstechnik 824, 2001.
- [8] I. Mangerig, *Klimatische Temperaturbeanspruchung von Stahl- und Stahlverbundbrücken*, Institut für Konstruktiven Ingenieurbau, Ruhr-Universität Bochum, Mitteilung Nr. 86-4, 1986.
- [9] U. Lichte, *Klimatische Temperatureinwirkungen und Kombinationsregeln bei Brückenbauwerken*, Dissertation, München, Germany, 2005.
- [10] N. Fouad, *Numerical Simulation of the Enviromental thermal Loadings of Structures*, Fraunhofer-IRB, 1998.
- [11] Bundesministerium für Verkehr, Bau und Stadtentwicklung (BMVBS), *Richtlinie zur Nachrechnung von Straßenbrücken im Bestand (Nachrechnungsrichtlinie)*, Berlin, 2011.
- [12] S. Marx, C. von der Haar, J.P. Liebig, J. Grünberg, Identification of traffic loads by measurements at expansion joints, *Bautechnik* 90(8), 466-474, 2013.
- [13] P. Lubasch, M. Schnellenbach-Held, W. Buschmeyer, Computer-Aided Identification of Traffic Loads-Supplemented Structural Health Monitoring, *Der Bauingenieur* 86(10), 433-442, 2011.
- [14] U.H. Clorman, T. Seeger, Rainflow-HCM - A counting method for fatigue strength evaluation based on material behaviour, *Stahlbau* 55 (3), 65–71, 1986.
- [15] EN 1991-2:2010, *Eurocode 1: Actions on structures – Part 2: Traffic loads on bridges*, 2010.
- [16] EN 1992-1-1:2011, *Eurocode 2: Design of concrete structures – Part 1-1: General rules and rules for buildings*, 2011.